

## Microstructure evolution and mechanical properties of AZ80 alloy reheated from as-cast and deformed states

ZHAO Gao-zhan<sup>1</sup>, YANG Lin<sup>2</sup>, DUAN Xun-xing<sup>2</sup>, REN Xiao-hua<sup>2</sup>, ZHU Li-min<sup>2</sup>,  
YANG Ting-jun<sup>2</sup>, GUO Xiang-yong<sup>2</sup>, HAO Shao-nan<sup>2</sup>

1. No.59 Institute of China Ordnance Industry, Chongqing 400039, China;
2. Chongqing Institute of Coal Science Research Institute, Chongqing 400037, China

Received 28 August 2012; accepted 25 October 2012

**Abstract:** Microstructure evolution and mechanical properties of AZ80 alloy reheated from the as-cast and deformed states were investigated. A new method, cyclic closed-die forging (CCDF), was employed to deformation of AZ80 as a recrystallization and partial melting (RAP) process. During partial remelting, finer, rounder and more homogeneous grains can be obtained from CCDF-formed alloys than from as-cast alloys. Prolonging isothermal holding time from 0 to 40 min, the mean grain size of solid particles in as-cast state decreased initially and then increased, however, that of CCDF-formed alloys increased continuously. The degree of spheroidization was improved in as-cast alloys with prolonging holding time. In contrast, in CCDF-formed alloys, the value of shape factor increased initially and then decreased. Microstructure evolution during remelting is dominated by many factors, for example distortion energy providing recrystallization driving force, Ostwald ripening mechanism, grain coalescence. Compared with the as-cast alloys, the CCDF-formed AZ80 alloy got a significant improvement in tensile properties. YS, UTS and elongation increased by 89%, 45% and 242% respectively. This can be mainly attributed to the grain refinement and elimination of defects.

**Key words:** AZ80 alloy; recrystallization; partial melting; cyclic closed-die forging; spheroidization; aggregation

### 1 Introduction

Semi-solid processing was established as a high-volume, near-net shape manufacturing process for components in the trade of mechanism producing, electronic part and aviation [1–3]. Compared with the traditional cast materials, billets formed by semi-solid processing have less segregation and porosity, and therefore have better mechanical properties. Because a globular microstructure of solid is needed and will exert a significant influence on the mechanical properties of products formed by semi-solid processing, the production of semi-solid billets is very important [4–6].

The required globular microstructure can be obtained by a number of routes. Solid-state routes include the strain-induced melt activation (SIMA) process and the recrystallization and partial melting (RAP) process [7]. The SIMA process involves severe hot working producing directional grain structure in the alloy. A critical level of strain must be introduced into the alloy either as an integral part of the hot working, or by

cold working as a separate step subsequent to the hot working, prior to heating to above the solidus temperature [8,9]. The RAP route involve working, e.g. extrusion, below the recrystallization temperature followed by reheating to the semi-solid state [10]. LIN et al reported the effect of pre-deformation on the globular grains in AZ91D alloy as a result of the SIMA process. They found that the pre-deformation refined the  $\alpha$ -Mg grains in the semi-solid microstructure due to the recrystallization mechanism, and further improved the tensile properties due to the refinement strengthening mechanism [11]. JI et al [12,13] reported the formation process of AZ31B semi-solid microstructures through the SIMA method. They found that increasing the heating temperature could accelerate the spheroidizing process, resulting in semi-solid microstructures containing small spheroidal particles; with a longer holding time in the vicinity of 883–893 K, the solid content slightly changed and the solid particles became irregular in shape.

In this work, a new method called cyclic closed-die forging (CCDF) was employed to deformation of AZ80 magnesium alloy in the RAP route. The microstructure

evolution and mechanical properties of the material reheated for different holding time were investigated, both in the as-cast and deformed states. In addition, the coarsening kinetics under the two states in the semi-solid state was also studied.

## 2 Experimental

Before experiment, as-cast AZ80 alloy ingots were prepared from outsourcing, with the measured composition (mass fraction) of 8.9% Al, 0.53% Zn and 0.25% Mn. Firstly, CCDF was employed to predeform a portion of as-cast AZ80 ingots, and the principle of the CCDF process is represented schematically in Fig. 1. A billet was first compressed in the vertical direction and then in the horizontal direction. The equivalent strain per operation is given by

$$\varepsilon_e = 2n \frac{\ln(H/W)}{\sqrt{3}} \quad (1)$$

where  $\varepsilon_e$  is the equivalent strain imposed by the CCDF die configuration,  $n$  is the number of CCDF passes,  $W$  and  $H$  are the width and height of the specimen, respectively [14,15]. Before CCDF, the as-cast AZ80 ingots were machined into a billet with a dimension of 80 mm×80 mm×160 mm. This as-cast billet was held at 380 °C for 40 min and then was processed through the closed die preheated to 380 °C, with a speed of 2 mm/s. Molybdenum disulphide (MoS<sub>2</sub>) was used as a lubricant during CCDF. Before each pass, the as-cast billet was heated at 380 °C for 6 min. The billet was processed for 4 passes, and then air cooled to room temperature.

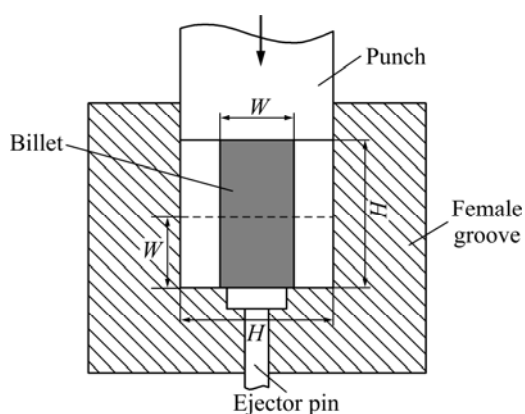


Fig. 1 Schematic of cyclic closed-die forging (CCDF)

The microstructure evolution during partial remelting in the semi-solid state was investigated on as-cast and four-pass CCDF-formed AZ80 cylindrical samples of  $d8\text{ mm}\times 12\text{ mm}$ , respectively. These samples were heated to semi-solid temperature of 570 °C in a furnace under a protective gas flow (Ar atmosphere), isothermally held and quenched in cold water. The

furnace temperature was controlled by a thermocouple placed next to the sample being isothermally held. Samples were heat treated isothermally at 570 °C for 0–40 min.

For the thixoforming, slugs with size of  $d80\text{ mm}\times 120\text{ mm}$  were cut from as-cast and CCDF-formed billets. The slugs were rapidly induction heated in the semi-solid region and then thixoformed into a die. The heating of the slug was monitored by using two K-type thermocouples embedded in the slug. The die was preheated to 400 °C and the billets were preheated at 570 °C for 10 min. During thixoforming, the punch speed was about 10 cm/s. The pressure exerted by the punch on the slug was gradually increased to a pre-determined level of 200 MPa and kept for 60 s.

Samples after partial remelting were hot mounted in conductive phenolic resin and prepared for optical microscopy using standard metallographic techniques. The remelted samples from as-cast were etched with 4% HNO<sub>3</sub> aqueous solution and those from CCDF were etched with a solution of 100 mL ethanol, 6 g picric acid, 5 mL acetic acid and 10 mL water. The microstructure of samples was studied and analyzed using optical microscopy. Grain size was measured from the resulting microstructures using an image analysis system [16,17]. Samples for tensile testing were machined from the thixoformed components and were tested using an Instron 5569 testing machine at a crosshead speed of 0.5 mm/min. The tensile samples had a gauge length of 15 mm and a thickness of 2 mm. Each tensile value was the average of at least three measurements.

## 3 Results and discussion

### 3.1 Microstructures of as-cast and CCDF-formed AZ80 alloys

Figure 2 shows the microstructures of as-cast and CCDF-formed AZ80 alloys. As shown in Fig. 2(a), the microstructure of as-cast AZ80 alloy consisted of the matrix ( $\alpha$ -Mg) and the intermetallic phase ( $\beta$ -Mg<sub>17</sub>Al<sub>12</sub>). The intermetallic phase was thick, semi-continuous or continuous net-like and mainly distributed at grain boundaries. However, an obvious directional band grains appear in Fig. 2(b) along the deformation direction after being CCDF-formed. The grain boundaries were not clear and the net-like  $\beta$ -Mg<sub>17</sub>Al<sub>12</sub> was broken into small particles distributed in the matrix. Obviously, the CCDF-formed grains were unrecrystallized and the materials can therefore be classified as being consistent with the RAP process.

### 3.2 Microstructures of as-cast and CCDF-formed AZ80 alloys during remelting

Figures 3 and 4 show the microstructures of as-cast

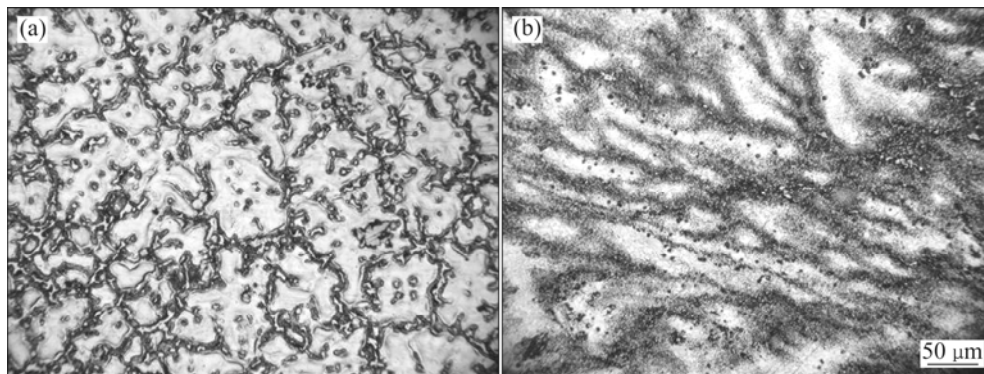


**Fig. 2** Microstructures of as-cast (a) and CCDF-formed (b) AZ80 magnesium alloy

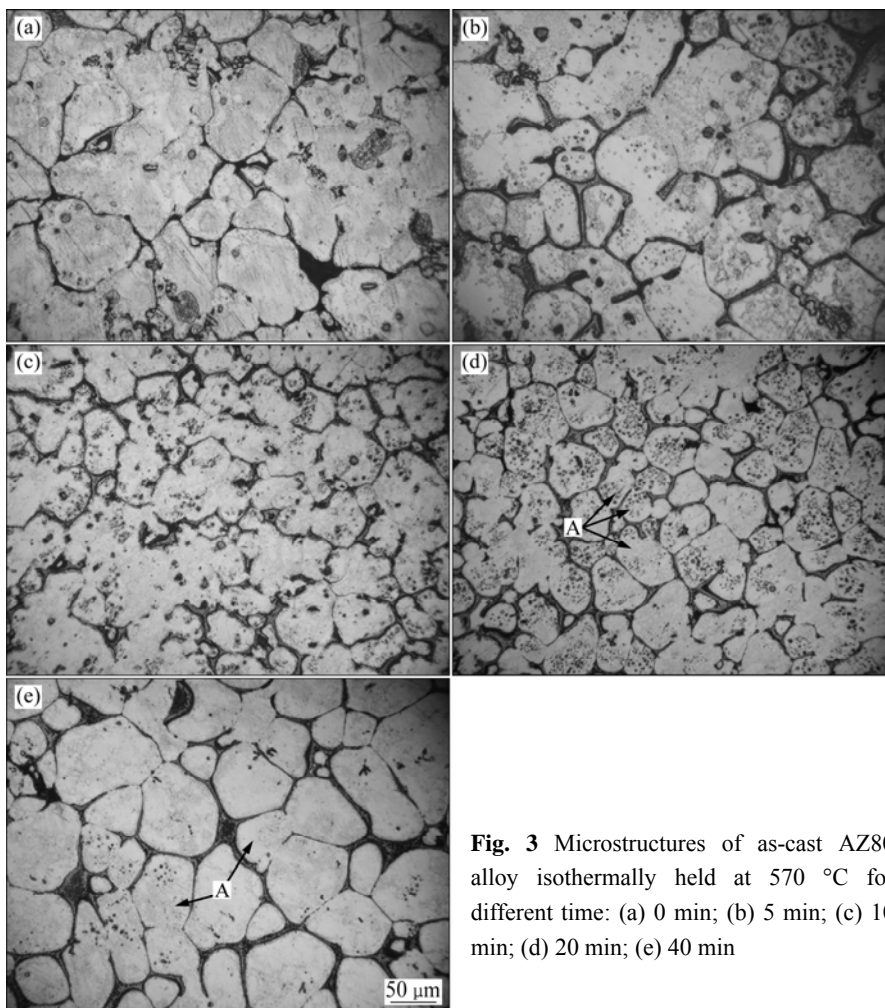


**Fig. 3** Microstructures of as-cast AZ80 alloy isothermally held at 570 °C for different time: (a) 0 min; (b) 5 min; (c) 10 min; (d) 20 min; (e) 40 min

and CCDF-formed AZ80 alloy isothermally held at 570 °C for different time. Figure 5 shows their mean grain size and shape factor as function of the holding time.

As shown in Fig. 3(a), when the sample was heated to 570 °C from as-cast state, grains appeared coarse and nonuniform obviously. When the sample was heated to 570 °C, solid particles had just began to be penetrated by the thin grain boundary liquid films. Prolonging isothermal holding time to 5, 20 and 40 min resulted in

the entire separation of contacted solid particles gradually due to thickening of liquid films (Fig. 3(b)) and increase in the amount of liquid fraction. Close examination of the microstructure (Figs. 3(a–e)) revealed that solid particles had undergone a significant degree of spheroidization during isothermal holding from 0 to 40 min. However, the mean grain size decreased initially (0 to 20 min) and then increased (20 to 40 min), as the holding time increased.

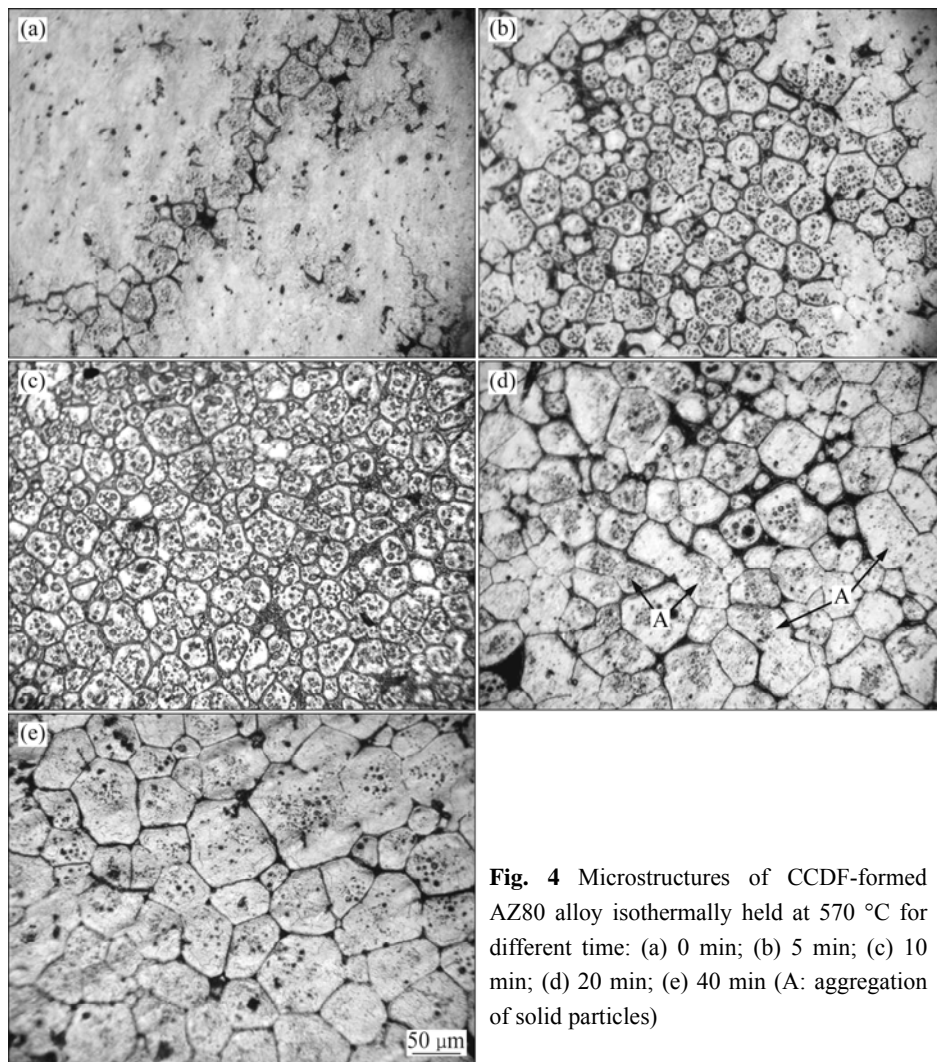


**Fig. 4** Microstructures of CCDF-formed AZ80 alloy isothermally held at 570 °C for different time: (a) 0 min; (b) 5 min; (c) 10 min; (d) 20 min; (e) 40 min (A: aggregation of solid particles)

As shown in Fig. 4(a), without isothermal holding at 570 °C, it was not enough for the spheroidization of solid particles and most of them were not penetrated by grain boundary liquid films. Moreover, partial remelting occurred in certain areas while other regions were still fully solid. With the isothermal holding continuing, the grain boundary liquid film thickened little by little, and the partial remelted areas spread to the whole microstructure of the CCDF-formed sample. Figure 4(c) shows the microstructure after 10 min isothermal holding at 570 °C. It can be seen that the relatively small, homogeneous and globular solid particles were obtained, but as the remelting continued, the solidified microstructure would be coarsened severely. Meanwhile, from Fig. 5, during remelting its mean grain size increased continuously from 35 μm to 94 μm, and the degree of spheroidization increased at the beginning of isothermal holding to 10 min, but then decreased from 10 min to 40 min. In addition, compared Fig. 3 with Fig. 4, it is seen that the microstructure from CCDF-formed state was obviously finer and more homogeneous than

from as-cast nearly at each stage of isothermal holding. Also, this features can be seen from Fig. 5.

### 3.3 Mechanisms of microstructure evolution during remelting

CCDF deformation can bring smaller solid particle size for AZ80 alloy as compared with as-cast state, but also bring the grain growth over time during isothermal holding. The increment of CCDF deformation increases the distortion energy stored in the forms of vacancies, lattice defect and dislocation multiplication, which can provide the driving force for the recovery and recrystallization during heating below solidus temperature and result in both grain nucleation and growth [18]. The more the amount of stored energy, the smaller the recrystallized grain size [19]. During CCDF deformation, due to 50% reduction in height per compression, the punch imposed the equivalent strain ( $\varepsilon_e$ ) of 3.2 on the billet according to Eq. (1) after four CCDF passes, which was stored in the form of distortion energy. However, the increment of nucleation rate is

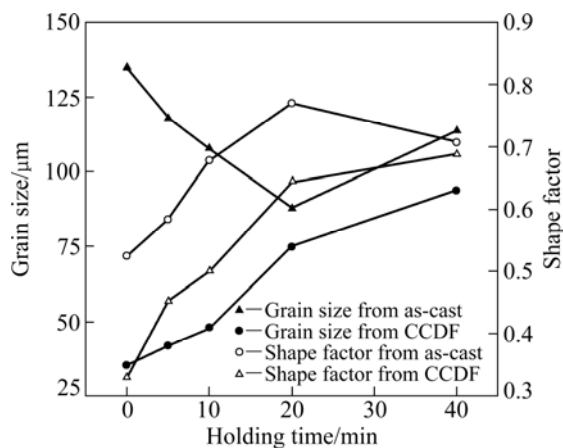


**Fig. 5** Mean grain size and shape factor of AZ80 alloy during isothermal holding at 570 °C for different time from as-cast and CCDF-formed states

faster than that of the growth rate. Two possible explanations are proposed for this. Firstly, the distortion energy and dislocation decrease as recrystallization proceeds, resulting in a reduction in the driving force [20]. After four passes of CCDF-deformation, distortion energy stored in the alloys is relatively low. With the consumption of limited distortion energy, recrystallization cannot be maintained. Secondly, the coarse and irregular recrystallized grains tend to aggregate in the relatively lower energy grain boundaries [21]. Under the condition of aggregation, two or more solid particles in contact with each other form a new solid particle with large size and irregular shape. It is evident from Fig. 3 and Fig. 4 that some aggregations of solid particles are clearly seen, as labelled A. Obvious aggregation became the dominant factor after the CCDF-deformed energy was run out.

A possible reason for the formation of irregularly shaped grains by grain coalescence can be shown in Fig. 6. A small spheroidal grain contacts with a large spheroidal grain and they merge into a larger grain. With increase in holding time, the larger grain gradually becomes spheroidal by slight reduction in solid–liquid interfacial energy [22], as shown in Fig. 6(a). However, when two spheroidal grains which are similar in size merge into a larger grain, with increase holding time, it is difficult for the irregular shape grain to become spheroidal owing to the low driving force, as shown in Fig. 6(b).

Figure 5 shows that with increasing holding time at 570 °C, the shape factor of AZ80 alloy at both as-cast and CCDF-formed states was improved gradually, but that of the CCDF-formed dropped after holding for 10 min. During partial remelting, the recrystallization first occurred. The growth of an expanding new grain during primary recrystallization led to an overall decrease in the

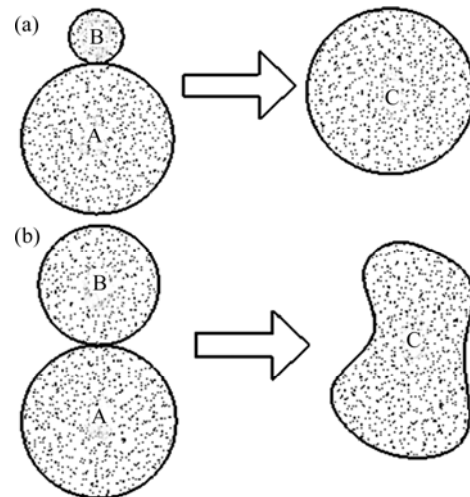


**Fig. 6** Schematic of grain aggregation: (a) Two with very different size merge into one; (b) Two with similar size merge into one

internal energy of the alloy by replacing deformed regions with strain-free regions [23]. The recrystallized grains were gradually surrounded by liquid film. With increasing in holding time, the liquid film became thicker. This reduced the probability of grain contacting with each other. In this condition, the recrystallized grains gradually changed to a round shape [24]. According to solidifying thermodynamics, the equilibrium melting point is connected with the interface energy:

$$\Delta T_r = -\frac{2T_m V_s \sigma K}{\Delta H_m} \quad (2)$$

where  $\Delta T_r = (T_m - T)$ , is the decrease in equilibrium melting point;  $T_m$  is the equilibrium transformation temperature;  $V_s$  is the solid mole volume;  $K$  is the mean surface curvature of the solid;  $\sigma$  is the interfacial tension and  $\Delta H_m = (H_s - H_l)$  is the molar change in enthalpy of the solid and liquid [25,26]. Hence, when the specimen is reheated to semi-solid temperature interval, the concave parts of the recrystallized grain are easy to melt than the bulge parts, and then the recrystallized grain gradually becomes round. Another key reason is that small solid particles and sharp corners of the big solid particles melt more quickly because their bigger curvatures bring lower melting point, which is also called Ostwald ripening mechanism [27,28]. Also, when spheroidization is completed, grain is coarsened by decrease in liquid/solid interfacial energy. In this condition, when liquid fraction is a constant, the thickness of liquid film gradually decreases along with increasing the grain size. When the recrystallized grains are not completely surrounded by liquid film, two grains contact with each other [29]. Because of the relatively uniform size of them, a new grain is merged into larger size, irregular-shaped one, as shown in Fig. 6.

### 3.4 Mechanical properties

Figure 7 presents a photograph of successfully thixoformed components. The component of starting materials was AZ80 magnesium alloy produced by the RAP route (four-pass CCDF plus partial remelting). The results indicated that the thixoformed components had a very good surface and no problem was experienced in filling the walled sections.



**Fig. 7** Thixoformed barrel-shaped components with thin walls by RAP route (four-pass CCDF and partial remelting)

Table 1 shows the mechanical properties of the thixoforged AZ80 components in comparison with those of as-cast and CCDF-formed samples. As shown in Table 1, the tensile properties of the thixoforged components of CCDF-formed samples show a significant improvement over those of as-cast ones. The increase of YS, UTS and elongation reach about 89%, 45% and 242% respectively.

**Table 1** Mechanical properties of thixoforged AZ80 components under two routes

Route	YS/MPa	UTS/MPa	Elongation/%
As-cast	105	205	3.8
CCDF	198	297	13

This could be mainly attributed to the finer grains by CCDF deformation and partial remelting, and the YS of the magnesium alloy has a strong dependence on grain size [30]. However, the UTS is also determined by the amount of defects present in the sample. The major defects affecting UTS are gas holes and shrinkage cavity [31]. The more the number of defects is, the lower the UTS and the elongation are. Because of CCDF deformation, these defects can be eliminated to some extent, which leads to higher strength and elongation as compared with as-cast samples.

## 4 Conclusions

CCDF followed by partial remelting is an effective route to produce semi-solid AZ80 magnesium alloy for thixoforging. It can break the net-like  $\beta$ -Mg<sub>17</sub>Al<sub>12</sub> in as-cast alloy into small particles distributed in the matrix and impose equivalent strain to grains.

During partial remelting, finer, rounder and more homogeneous grains can be obtained from CCDF-formed state than from as-cast state. Prolonging the isothermal holding time from 0 to 40 min, the mean grain size of solid particles from as-cast state decreased initially and then increased, while it increased continuously from CCDF state. The value of spheroidization from as-cast state increased continuously, while CCDF increased initially and then decreased from CCDF state.

Microstructure evolution during remelting is dominated by many factors such as distortion energy providing recrystallization driving force, Ostwald ripening mechanism, grain coalescence and so on.

Compared with the as-cast state, the tensile properties of the CCDF-formed AZ80 alloy get a significant improvement. The YS, UTS and elongation increase by about 89%, 45% and 242% respectively.

## References

- [1] ZHAO Zu-de, CHEN Qiang, WANG Yan-bin, SHU Da-yu. Effect of predeformation on semi-solid microstructure of ZK60+RE magnesium alloy [J]. Transactions of Nonferrous Metals Society of China, 2009, 19: 535–539.
- [2] HU Hong-jun, ZHANG Ding-fei, PAN Fu-sheng. Die structure optimization of equal channel angular extrusion for AZ31 magnesium alloy based on finite element method [J]. Transactions of Nonferrous Metals Society of China, 2010, 20(2): 259–266.
- [3] ZHAO Zu-de, CHEN Qiang, HU Chuan-kai, SHU Da-yu. Microstructure and mechanical properties of SPD-processed an as-cast AZ91D+Y magnesium alloy by equal channel angular extrusion and multi-axial forging [J]. Materials and Design, 2009, 30: 4557–4561.
- [4] LUO Shou-jing, CHEN Qiang, ZHAO Zu-de. Effects of processing parameters on the microstructure of ECAE-formed AZ91D magnesium alloy in the semi-solid state [J]. Journal of Alloys and Compounds, 2009, 477: 602–607.
- [5] ZHAO Zu-de, CHEN Qiang, KANG Feng, SHU Da-yu. Microstructural evolution and tensile mechanical properties of thixoformed AZ91D magnesium alloy with the addition of yttrium [J]. Journal of Alloys and Compounds, 2009, 482: 455–467.
- [6] THIRUMURUGAN M, THIRUGNASAMBANDAM G M, KUMARAN S, SRINIVASA RAO T. Microstructural refinement and mechanical properties of direct extruded ZM21 magnesium alloys [J]. Transactions of Nonferrous Metals Society of China, 2011, 21(10): 2154–2159.
- [7] ZHAO Zu-de, CHEN Qiang, WANG Yan-bin, SHU Da-yu. Microstructural evolution of an ECAE-formed ZK60-RE magnesium alloy in the semi-solid state [J]. Materials Science and Engineering A, 2009, 506: 8–15.
- [8] CHEN Qiang, LIN Jun, SHU Da-yu, HU Chuan-kai, ZHAO Zu-de, KANG Feng, HUANG Shu-hai, YUAN Bao-guo. Microstructure development, mechanical properties and formability of Mg–Zn–Y–Zr magnesium alloy [J]. Materials Science and Engineering A, 2012, 554: 129–141.
- [9] CHEN Qiang, LUO Shou-jing, ZHAO Zu-de. Microstructural evolution of previously deformed AZ91D magnesium alloy during partial remelting [J]. Journal of Alloys and Compounds, 2009, 477: 726–731.
- [10] ZHAO Zu-de, CHEN Qiang, WANG Yan-bin, SHU Da-yu. Microstructures and mechanical properties of AZ91D alloys with Y addition [J]. Materials Science and Engineering A, 2009, 515:

- 152–161.
- [11] LIN Hua-qiang, WANG Jin-guo, WANG Hui-yuan, JIANG Qi-chuan. Effect of predeformation on the globular grains in AZ91D alloy during strain induced melt activation (SIMA) process [J]. Journal of Alloys and Compounds, 2007, 431: 141–147.
- [12] JI Ze-sheng, HU MAO-lian, SUGIYAMA S, YANAGIMOTO J. Formation process of AZ31B semi-solid microstructures through SIMA method [J]. Mater Charact, 2008, 59: 905–911.
- [13] LUO Shou-jing, CHEN Qiang, ZHAO Zu-de. An investigation of microstructure evolution of RAP processed ZK60 magnesium alloy [J]. Materials Science and Engineering A, 2009, 501: 146–152.
- [14] CHEN Qiang, HUANG Zhi-wei, ZHAO Zu-de, HU Chuan-kai, SHU Da-yu. Thermal stabilities, elastic properties and electronic structures of B2-MgRE (RE=Sc, Y, La) by first-principles calculations [J]. Computational Materials Science, 2013, 67: 196–202.
- [15] HE Yun-bin, PAN Qing-lin, CHEN Qin, LIU Xiao-yan, LI Wen-bin. Modeling of strain hardening and dynamic recrystallization of ZK60 magnesium alloy during hot deformation [J]. Transactions of Nonferrous Metals Society of China, 2012, 22(5): 1255–1261.
- [16] LUO Shou-jing, CHEN Qiang, GAO Xiao-rong. Mechanical analysis of semi-solid metals shear deformation during compression [J]. Semi-Solid Processing of Alloys and Composites X, 2008, 7: 439–443.
- [17] ZHAO Zu-de, CHEN Qiang, TANG Ze-jun, HU Chuan-kai. Microstructural evolution and tensile mechanical properties of AM60B magnesium alloy prepared by the SIMA route [J]. Journal of Alloys and Compounds, 2010, 497: 402–411.
- [18] ZHANG Ding-fei, SHI Guo-liang, ZHAO Xia-bing, QI Fu-gang. Microstructure evolution and mechanical properties of Mg-x%Zn-1%Mn (x=4, 5, 6, 7, 8, 9) wrought magnesium alloys [J]. Transactions of Nonferrous Metals Society of China, 2011, 21(1): 15–25.
- [19] ZHAO Zu-de, CHEN Qiang, CHAO Hong-ying, HUANG Shu-hai. Microstructural evolution and tensile mechanical properties of thixoforged ZK60-Y magnesium alloys produced by two different routes [J]. Materials and Design, 2010, 31: 1906–1916.
- [20] CHENG Yuan-sheng, CHEN Qiang, HUANG Zhe-qun, HUANG Shu-hai. Microstructure evolution and thixoextrusion of AZ91D magnesium alloy produced by SSTT [J]. Transactions of Nonferrous Metals Society of China, 2010, 20: s739–s743.
- [21] ZHAO Zu-de, CHEN Qiang, HUANG Shu-hai, KANG Feng, WANG Yanbin. Microstructure and tensile properties of AM50A magnesium alloy prepared by recrystallisation and partial melting process [J]. Transactions of Nonferrous Metals Society of China, 2010, 20: 1630–1637.
- [22] LIU Zheng, MAO Wei-min, LIU Xiao-mei. Effect of pouring temperature on fractal dimension of primary phase morphology in semi-solid A356 alloy [J]. Transactions of Nonferrous Metals Society of China, 2009, 19(5): 1098–1103.
- [23] ZHAO Zu-de, CHEN Qiang, TANG Ze-jun, WANG Yan-bin, NING Hai-qing. Microstructure evolution and mechanical properties of Al<sub>2</sub>O<sub>3</sub>/AZ91D magnesium matrix composites fabricated by squeeze casting [J]. Journal of Materials Science, 2010, 45: 3419–3425.
- [24] CHEN Qiang, SHU Da-yu, HU Chuan-kai, ZHAO Zu-de, YUAN Bao-guo. Grain refinement in an as-cast AZ61 magnesium alloy processed by multi-axial forging under the multitemperature processing procedure [J]. Materials Science and Engineering A, 2012, 541: 98–104.
- [25] ZHAO Zu-de, CHENG Yuan-sheng, CHEN Qiang, WANG Yan-bin, SHU Da-yu. Reheating and thixoforging of ZK60+RE alloy deformed by ECAE [J]. Transactions of Nonferrous Metals Society of China, 2010, 20: 178–182.
- [26] YU Kun, RUI Shou-tai, WANG Xiao-yan, WANG Ri-chu, LI Wen-xian. Texture evolution of extruded AZ31 magnesium alloy sheets [J]. Transactions of Nonferrous Metals Society of China, 2009, 19(3): 511–516.
- [27] ZHAO Zu-de, CHEN Qiang, CHAO Hong-ying, HU Chuan-kai, HUANG Shu-hai. Influence of equal channel angular extrusion processing parameters on the microstructure and mechanical properties of Mg–Al–Y–Zn alloy [J]. Materials and Design, 2011, 32: 575–583.
- [28] CHEN Qiang, ZHAO Zhi-xiang, SHU Da-yu, ZHAO Zu-de. Microstructure and mechanical properties of AZ91D magnesium alloy prepared by compound extrusion [J]. Materials Science and Engineering A, 2011, 528: 3930–3934.
- [29] LI Yuan-dong, CHEN Ti-jun, MA Yin, YAN Feng-yun, HAO Yuan. Effect of rare earth 0.5% addition on semi-solid microstructural evolution of AZ91D alloy [J]. Transactions of Nonferrous Metals Society of China, 2007, 17(2): 320–325.
- [30] CHEN Qiang, SHU Da-yu, ZHAO Zu-de, ZHAO Zhi-xiang, WANG Yan-bin, YUAN Bao-guo. Microstructure development and tensile mechanical properties of Mg–Zn–RE–Zr magnesium alloy [J]. Materials and Design, 2012, 40: 488–496.
- [31] CHEN Qiang, ZHAO Zu-de, ZHAO Zhi-xiang, HU Chuan-kai, SHU Da-yu. Microstructure development and thixoextrusion of magnesium alloy prepared by repetitive upsetting-extrusion [J]. Journal of Alloys and Compounds, 2011, 509: 7303–7315.

## 铸态与变形态 AZ80 镁合金重熔后的组织演变和力学性能

赵高瞻<sup>1</sup>, 杨林<sup>2</sup>, 段勋兴<sup>2</sup>, 任晓华<sup>2</sup>, 朱利民<sup>2</sup>, 阳廷军<sup>2</sup>, 郭向勇<sup>2</sup>, 郝少楠<sup>2</sup>

1. 中国兵器工业第五九研究所, 重庆 400039;
2. 重庆煤炭科学研究院, 重庆 400037

**摘要:** 对铸态和变形态 AZ80 镁合金重熔后的组织演变与力学性能进行比较。将一种新的成形工艺——循环闭式模锻(CCDF)应用于 AZ80 再结晶局部重熔(RAP)的变形工艺中。相比铸态合金, CCDF 变形态可以获得更加细小、均匀、圆整的晶粒组织。随着等温热处理时间从 0 延长到 40 min, 铸态 AZ80 合金的晶粒呈现先细化后粗化的趋势, 而 CCDF 变形态则持续粗化。与此同时, 前者的圆整度持续增加, 而后者则先增后减。重熔过程中的组织演变是多种因素复合的结果, 如晶格畸变提供的再结晶驱动力、Ostwald 熟化机制以及晶粒合并长大机制等。与铸态相比, CCDF 变形态的力学性能明显改善, 屈服强度、抗拉强度以及伸长率增幅分别达到 89%、45%和 242%, 这主要得益于组织的细化与缺陷的消除。

**关键词:** AZ80 镁合金; 再结晶; 局部重熔; 循环闭式模锻; 球化; 合并

(Edited by YUAN Sai-qian)